SUPPLEMENTARY MATERIAL

Structural analysis of the B-box 2 from MuRF1:

Identification of a novel self-association pattern in a RING-like fold

Michael Mrosek[§], Sebastian Meier[§,&], Zöhre Ucurum-Fotiadis[§,&], Eleonore von Castelmur[§], Erik Hedbom[§], Ariel Lustig[§], Stephan Grzesiek[§], Dietmar Labeit[⊥], Siegfried Labeit[⊥], Olga Mayans[f,§,*]

[§]*Division of Structural Biology, Biozentrum, University of Basel, Klingelbergstrasse 70, CH-4056 Basel, Switzerland;* [⊥]*Institut für Anästhesiologie und Operative Intensivmedizin, Universitätsklinikum Mannheim, D-68167 Mannheim, Germany;* [f]*School of Biological Sciences, University of Liverpool, Crown Street, Liverpool L69 7ZB, UK*

Table S1: Interproton distances[a] (Å) in the crystallographic monomer of MuRF1 B2 (i), the non-crystallographic dimer in the asymmetric unit (ii) and a crystallographic lattice dimer (iii). Distances correlate with the NOE data shown in **Figure S8**.

	Q^{δ} F148			**Q^{ε} F148**		
	intra-monomer (i)	**dimer (ii)**	**dimer (iii)**	**intra-monomer (i)**	**dimer (ii)**	**dimer (iii)**
$Q^{\delta 1}$ I132	-	-	-	10.7	4.4	28.4
QQ^{γ} V156	11.2	4.6	28.2	11.9	2.6	28.9
$Q^{\gamma 2}$ I132	10.9	4.5	26.7	11.4	2.3	28.0
H^{γ} P158	15.7	3.7	28.7	15.5	3.6	29.2
H^{β} P158	15.6	4.5	26.7	15.6	3.9	27.9
Q^{δ} P158	16.2	3.8	27.7	16.4	3.0	28.7
H^{α} P158	14.8	5.1	26.3	15.1	3.3	27.5
H^{α} A157	16.0	4.4	28.6	16.5	2.4	29.5
QQ^{γ} V147	3.3	-	-	3.5	-	-
$H^{\beta 1}$ M144	4.6	-	-	-	-	-
H^{β} V147	3.2	-	-	3.6	-	-
$H^{\beta 2}$ M144	2.9	-	-	-	-	-
Q^{ε} M144	2.6	-	-	2.4	-	-
Q^{γ} M144	4.7	-	-	-	-	-
$H^{\beta 2}$ F148	2.7	-	-	4.8	-	-
$H^{\beta 1}$ F148	2.3	-	-	4.6	-	-
HA M144	3.2	-	-	4.2	-	-
HN V147	4.7	-	-	-	-	-
HN F148	3.3	-	-	-	-	-

[a]Atom groups of methylenes, methyls and phenylalanine ring protons, for which individual protons are not assigned individually, are denoted as pseudoatoms "Q" (*1*). For methylene and methyl groups the shortest distance is given between either of the methylene/methyl protons and either of the two equivalent tyrosine ring protons.

Figure S1: Sequence alignment of B2 boxes

Boxes of known structure are shown in bold; TRIM63 corresponds to MuRF1, TRIM18 to MID1, TRIM1 to MID2 and TRIM29 to ATDC.

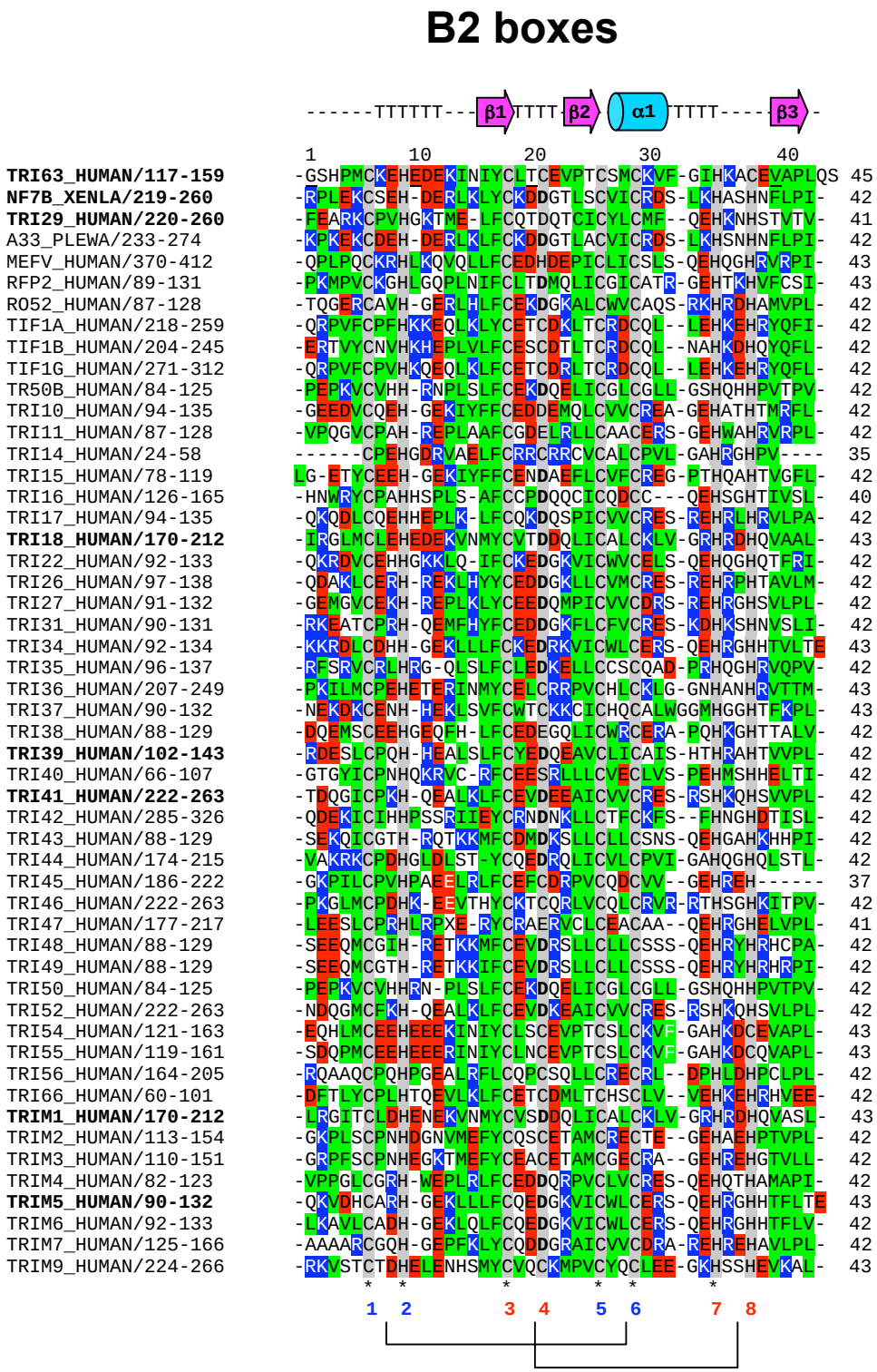

Figure S2: Comparison of crystallographic and NMR models of MuRF1 B2

a. Family of NMR conformers (PDB entry 2D8U); **b.** Superposition of the three molecular copies in the asymmetric unit of the crystal. It should be noted that non-crystallographic restraints were not applied to the refinement of these models; **c.** Superimposition of the crystallographic models (red) and the NMR family of conformers (grey). Although the overall agreement of the models in good, there are small displacements in the relative position of structural elements. Fitting of solution RDC data to the crystal structure indicates a clearly improved coordinate precision (Q=0.2) relative to the lowest energy conformer of 2D8U (Q=0.7).

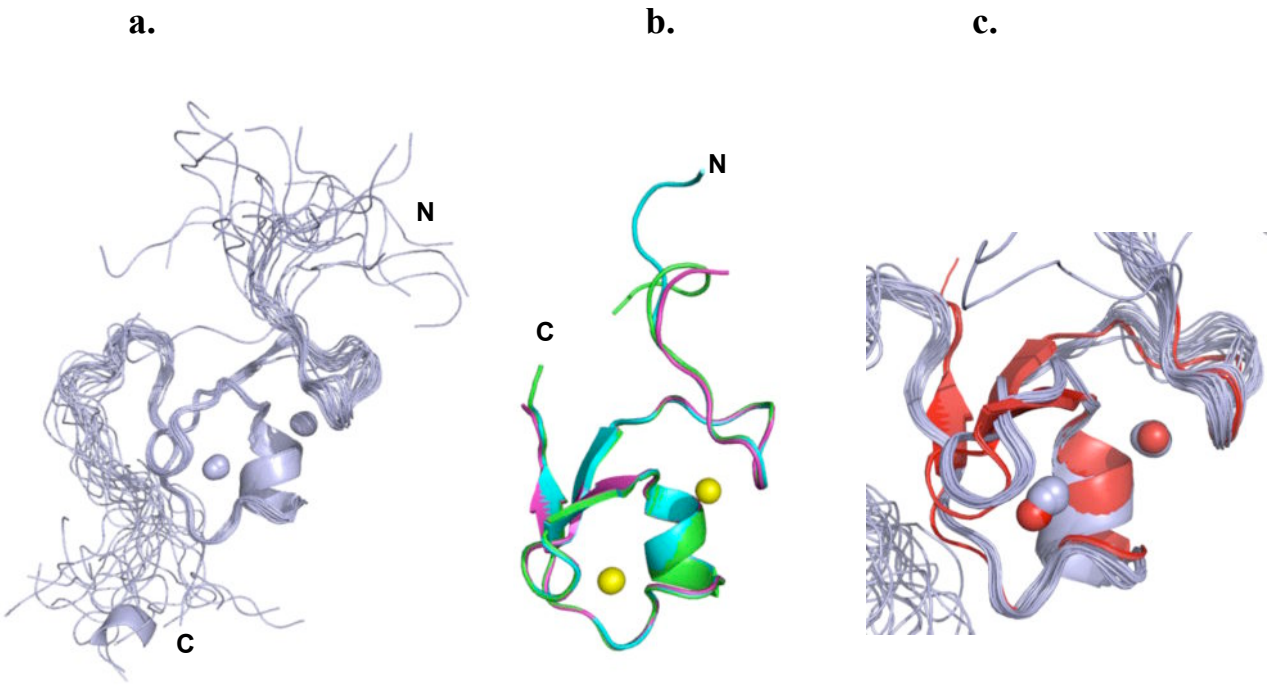

Figure S3: Interface residues

Stereo plots of the $(2F_{obs}-F_{cal})\alpha_{calc}$ electron density map contoured at 1.5σ level for several hydrophobic (**a**) and polar (**b**) interacting groups at the dimer interface.

a.

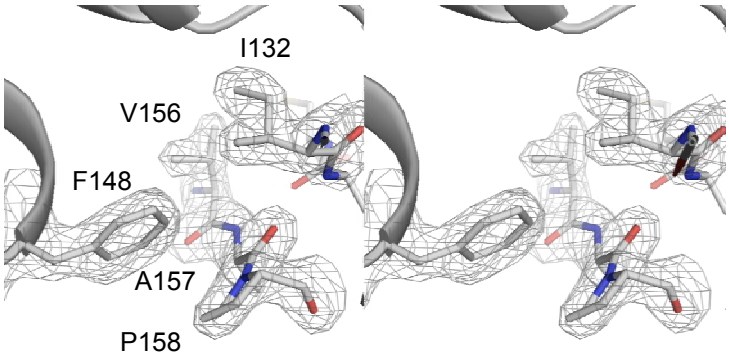

b.

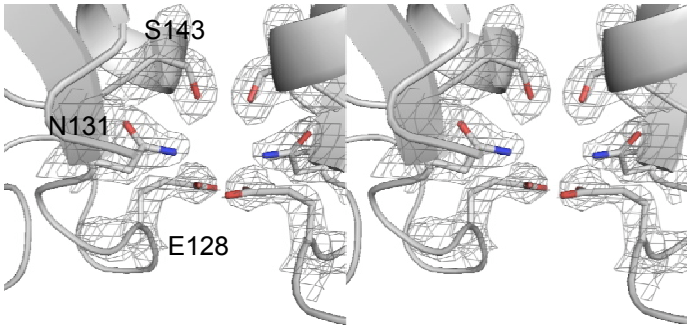

Figure S4: Relaxation data

$\{^{1}H\}$-^{15}N NOE, as well as ^{15}N T_1 and T_2 values of MuRF1 B2 recorded at a field strength of 14.1 T. Large-amplitude ps to ns dynamics is absent in the folded core between residues 121 and 159. Slower dynamics on the μs to ms timescale (K_{ex}, bottom left) is observed for several residues in the dimer interface (right), independent of assuming isotropic or anisotropic rotational diffusion tensor models. The interactions mediated by these residues (E128, K129, I132, M144 and F148) in dimerization are described in the main text.

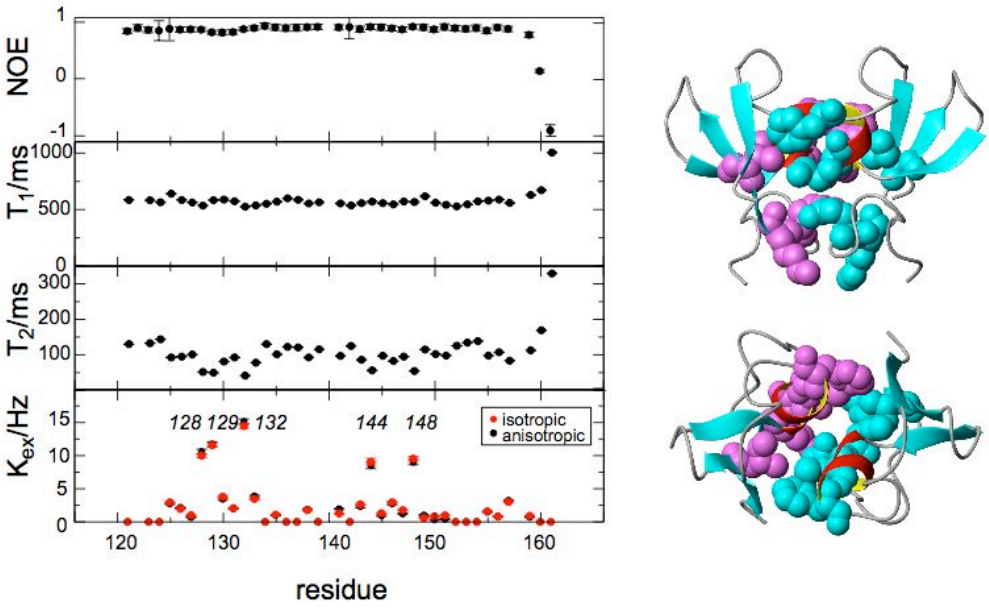

Figure S5: HSCQ NMR data

^{1}H-^{15}N HSQC spectrum of ^{15}N labelled MURF1 B2. One set of signals is obtained. ^{1}H and ^{15}N relaxation times show a correlation time of 6.4 ns, corresponding to a molecular weight of ~12 KDa and strongly indicative of a dimeric state in solution. Residues N-terminal of M121 are broadened beyond detection due to intermediate exchange on the chemical shift time scale.

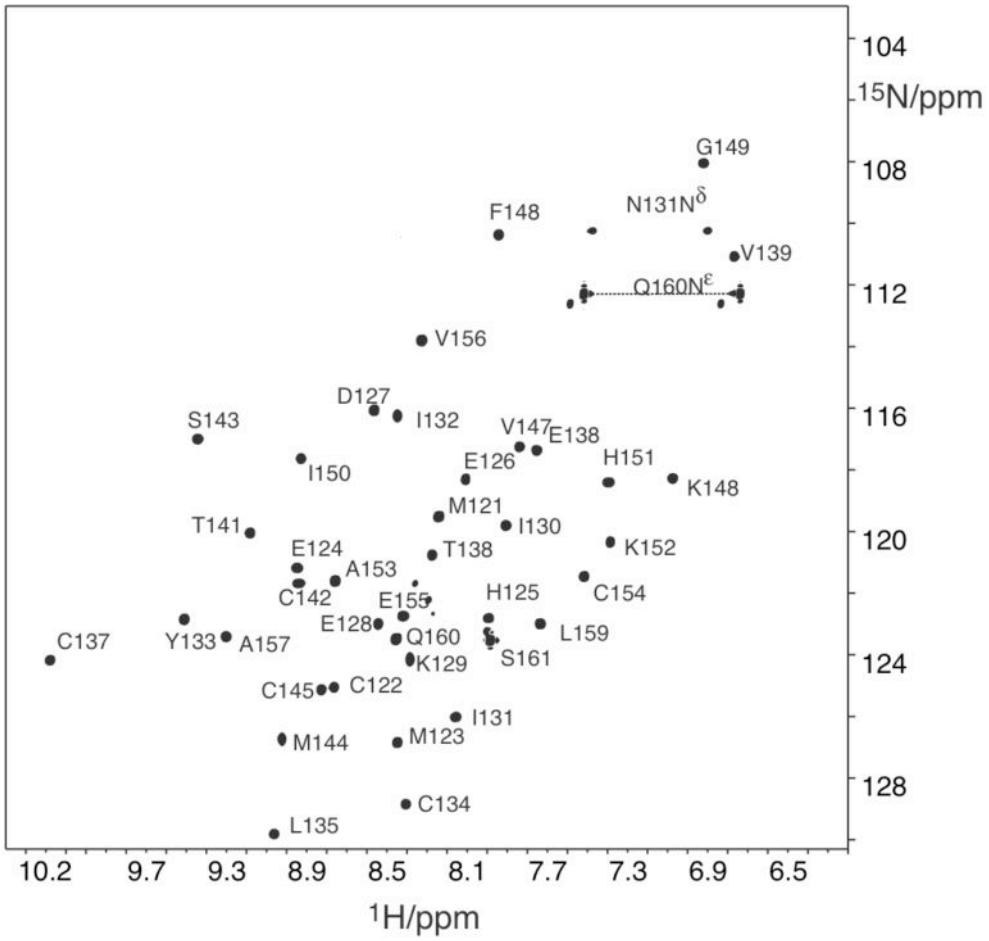

Figure S6: Comparative HSQC data on a diluted B2 sample

Superimposition of ^{1}H-^{15}N HSQC spectra of MuRF1 B2 at 3 mM and 0.3 mM (10-fold dilution) shows only minor changes in spectral appearance, suggesting that the sample remains predominantly in its dimeric state upon dilution.

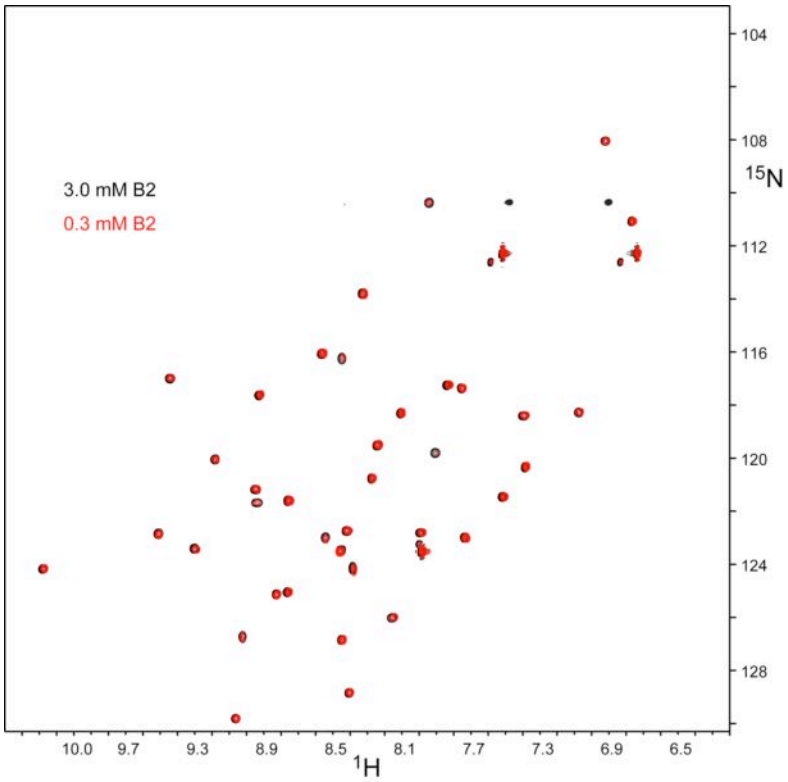

Figure S7: Dimeric forms of MuRF1 B2 in the crystalline lattice

a. The asymmetric unit of the crystal contains three polypeptidic chains of MuRF1 B2: chain A (cyan), chain B (green) and chain C (magenta); **b.** Chains A and B in the asymmetric unit form a non-crystallographic dimer, while chain C forms an equivalent dimer with a crystallographic copy of itself that obeys the crystal symmetry; **c.** The dimers formed by chains A-B and chains C-C' are identical. The presence of this dimeric form in solution has been confirmed using extensive NMR experiments.

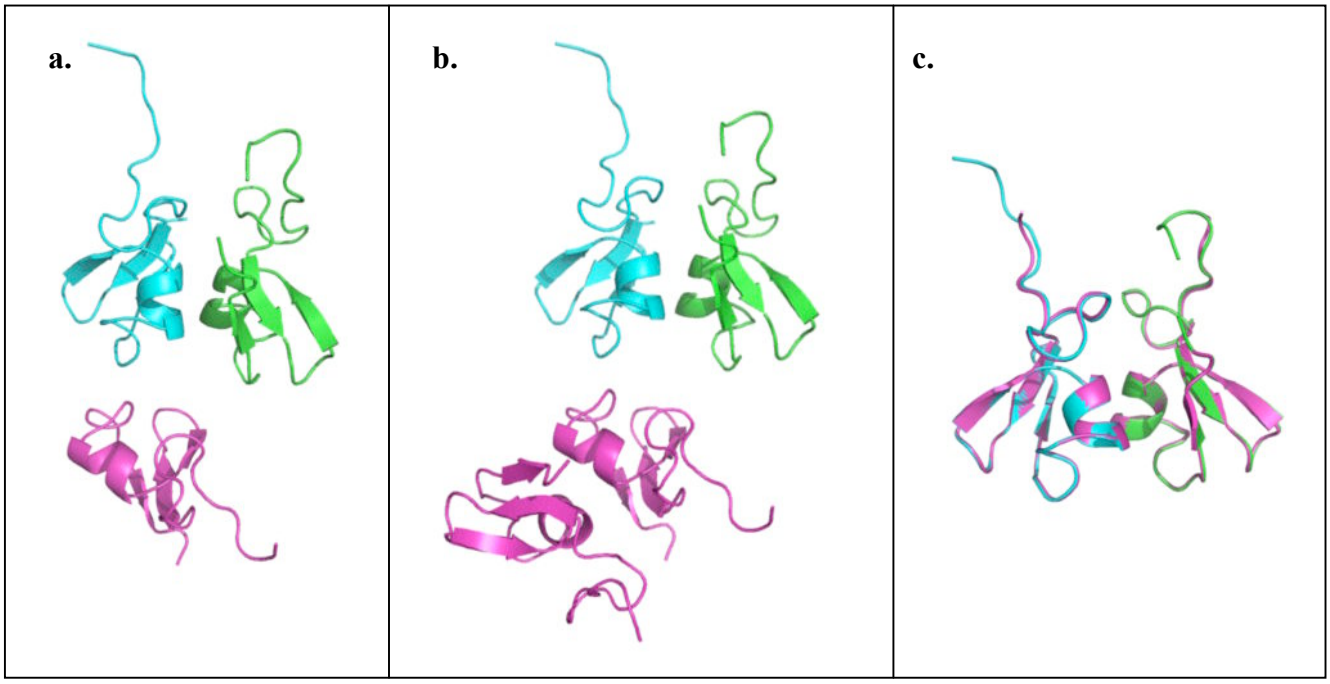

The crystallographic lattice, which by definition implies interactions across molecules in 3D, contained one other set of potential dimers. In this second form, each molecular copy in the asymmetric unit generates a dimer by packing against other crystallographic copies, namely chain A packs against a crystallographic copy of chain C and vice versa, while chain B packs against a crystallographic copy of itself (**d**). In this case,

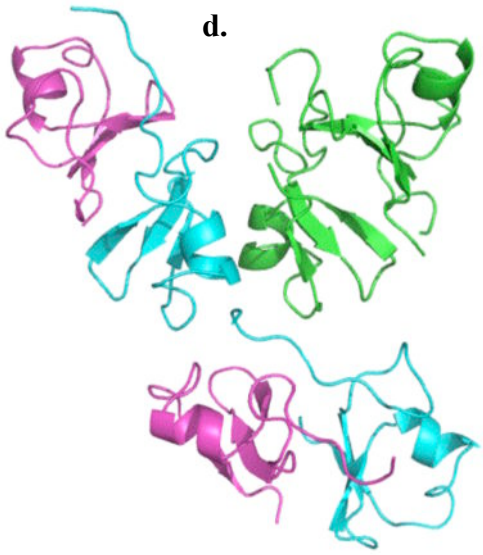

no dimer exists within the asymmetric unit of the crystal. This dimeric form could not be observed in solution using NMR measurements.

Figure S8: NOE data

Section of the NOESY spectrum recorded from a MuRF1 B2 sample at 3 mM concentration with a mixing time of 100 ms. NOEs to the δ and ε protons of phenylalanine 148 are shown. NOEs in red are explained by the crystal structure of the dimer as found in the asymmetric unit. Such NOEs cannot result from groups within the monomer alone since all corresponding distances are above 10.7 Å and, thus, would not lead to a detectable signal in NOESY spectra.

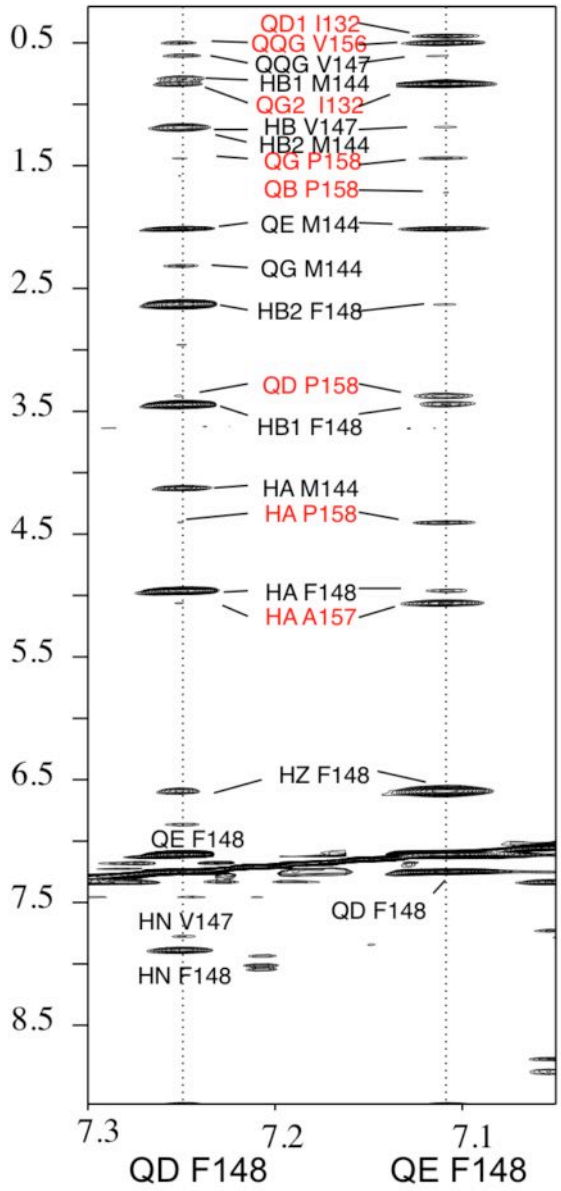

Figure S9: RDC data

Superimposition of ^{1}H-^{15}N IPAP segments for the measurement of RDCs in MURF1 B2. The domain was weakly oriented to give a maximal $^{1}D_{NH}$-RDC of 12.6 Hz upon the addition of Pf1 phages to a final concentration of 15 mg/ml and NaCl to a final concentration of 75 mM. A fit of RDCs obtained in this way strongly indicates that the dimeric arrangement of this domain in solution agrees with that present in the asymmetric unit of B2 crystals.

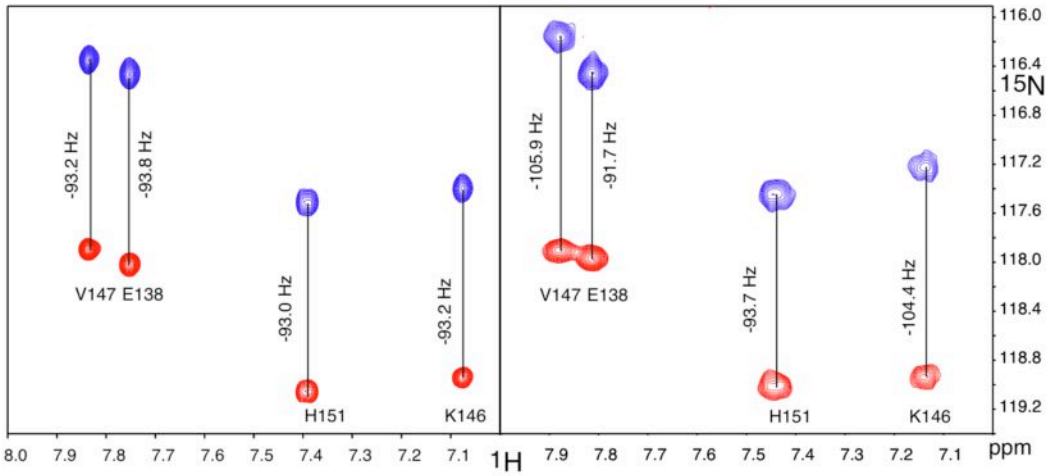

Figure S10: Comparative overview of RING-like motifs

a. Superposition of representative RING-like folds structurally characterized to date, namely MuRF1 B2, MID1 B1 (2FFW), U-box (2BAY), FYVE (1HYI), ZZ (1TOT), RING (1CHC), PHD (1F62), RING2 (1WD2). The shared structural core consisting of helix α1 and strands β1 and β2 is revealed (coloured). The most structurally similar region encompasses the metal site ZnI, while the architecture surrounding site ZnII is largely variable; **b.** Comparison of consensus sequences for the fold classes displayed in *a.* Metal binding residues are numbered and coloured according to the metal site they form. The position of hydrophobic residues is indicated by Θ and highlighted in yellow. It should be noted that in MuRF1 B2, hydrophobic residues do not form part of a motif core but that they are mainly solvent exposed. Other conserved residues within the classes are indicated. Consensus sequences for individual folds have been adapted from: RING and PHD domain (*2*); B1 (*3*); ZZ (*4*); FYVE (*5*); U-box (*6*).

a.

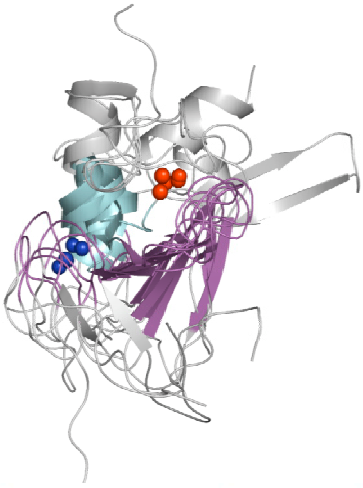

b.

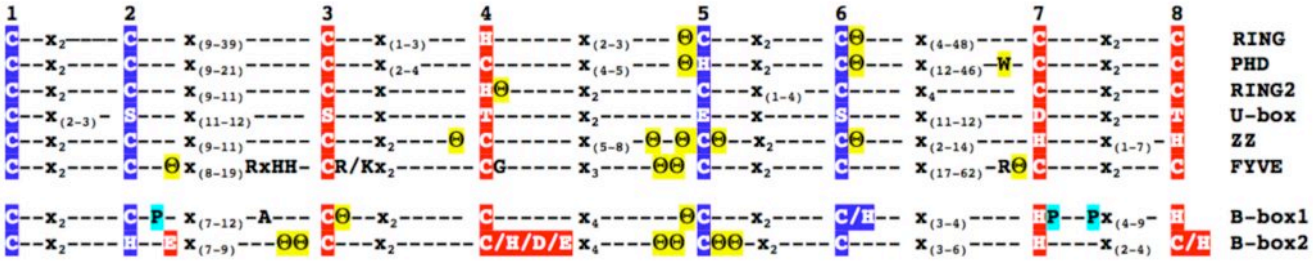

REFERENCES

1. Markley, J.L. Bax, A., Arata, Y., Hilbers, C.W., Kaptein, R., Sykes, B.D. Wright, P.E., and Wuthrich, K. (1998). Recommendations for the presentation of NMR structures of proteins and nucleic acids. IUPAC-IUBMB-IUPAB Inter-Union Task Group on the standarization of databases of protein and nucleic acid structures determined by NMR Spectroscopy. *J. Biomol. NMR 12*, 1-23.
2. Capili, A.D., Schultz, D.C., Rauscher, I.F., and Borden, K.L. (2001) Solution structure of the PHD domain from the KAP-1 corepressor: structural determinants for PHD, RING and LIM zinc-binding domains, *EMBO J 20*, 165-177.
3. Massiah, M.A., Simmons, B.N., Short, K.M., and Cox, T.C. (2006) Solution structure of the RBCC/TRIM B-box1 domain of human MID1: B-box with a RING. J Mol Biol, 358, 532-545.
4. Meroni, G. & Diez-Roux, G. (2005) TRIM/RBCC, a novel class of 'single protein RING finger' E3 ubiquitin ligases, *Bioessays 27*, 1147-1157.
5. Stenmark, H., Aasland, R., and Driscoll, P.C. (2002) The phosphatidylinositol 3-phosphate-binding FYVE finger, *FEBS Lett. 513*, 77-84.
6. Ohi, M.D., Vander Kooi, C.W., Rosenberg, J.A., Chazin, W.J., and Gould, K.L. (2003) Structural insights into the U-box, a domain associated with multi-ubiquitination, *Nat. Struct. Biol. 10*, 250-255.